Calorimetric Studies of the Binding of Ferric Ions to Ovotransferrin and Interactions between Binding Sites†

Lung-Nan Lin,‡ Anne B. Mason,§ Robert C. Woodworth,§ and John F. Brandts*,‡

Department of Chemistry, University of Massachusetts, Amherst, Massachusetts 01003, and Department of Biochemistry, University of Vermont, Burlington, Vermont 05405

Received July 2, 1991; Revised Manuscript Received August 20, 1991

ABSTRACT: Transferrins are two-domain proteins with a very strong site for iron binding located in each domain. Using ultrasensitive titration calorimetry, the binding of ferric ion (chelated with a 2-fold molar excess of nitrilotriacetate) to the two sites of ovotransferrin was studied in detail as well as the binding to the single site in the N- and C-terminal half-molecules. In the presence of excess bicarbonate ion, the binding occurs in two kinetic steps. The fast process of *contact binding* is instantaneous with respect to instrument response time, is strongly exothermic for the N site and less so for the C site, and corresponds to binding of the chelated ferric ion. The slower process of *bicarbonate insertion* with concomitant release of nitrilotriacetate occurs on a time scale of 2–20 min over the temperature range 7–37 °C and is endothermic for the N site and exothermic for the C site, with rates being signifcantly slower for insertion at the C site. The ΔH of binding is strongly temperature-dependent for both sites, arising from a large negative ΔC_p of binding which probably indicates removal of hydrophobic groups from contact with water. When bicarbonate ion is absent, only the fast process of contact binding is seen. Each site within a half-molecule is qualitatively similar to the same site in intact ovotransferrin, although quantitative differences were detected. It was shown that contact binding to ovotransferrin occurs reversibly with free exchange of Fe^{+3} between N and C sites, while the attachment to either site becomes essentially irreversible after bicarbonate insertion. The strong preference for the first ferric ion to bind to the N site is shown to be due to its larger contact binding constant and the faster rate of bicarbonate insertion, relative to the C site, and is not due to stronger thermodynamic binding after bicarbonate insertion. True equilibrium is achieved only over much longer periods of time. In another series of experiments, direct binding studies were carried out between the two half-molecules under different states of ligation with Fe^{+3} in the presence of bicarbonate. The results indicate that the two binding sites in ovotransferrin, separated by ca. 40 Å, are not independent of one another but communicate as a result of ligand-dependent changes in the heats and free energies of domain–domain interactions. These changes in interactions are such that they increase the thermodynamic binding constant of ferric ion to the N site and decrease the binding constant to the C site, relative to the situation which would exist in the absence of interdomain signaling. This may or may not be advantageous in carrying out the physiological function of ovotransferrin.

The transferrins comprise a group of glycoproteins (ca. 80 kDa) found in the blood plasma of vertebrates down to the hemolymph of chordates (Harris & Aisen, 1989; Bartfeld & Law, 1990). These single-chain proteins consist of two genetically related domains (N and C lobes), each made up of a pair of subdomains which define a binding cleft capable of sequestering a high-spin ferric ion and a synergistic anion, normally bicarbonate (the final bound form is likely divalent carbonate) in the physiological situation (Bailey et al., 1988; Harris & Aisen, 1989; Anderson et al., 1989; Chasteen & Woodworth, 1990). Many small carboxylate anions containing a second electron-donor function can substitute for bicarbonate (Williams & Woodworth, 1973; Schlabach & Bates, 1975; Woodworth et al., 1975; Bailey et al., 1988; Anderson et al., 1989; Dubach et al., 1991). Preparation of half-molecules of transferrins either by proteolysis (Williams, 1974; Lineback-Zins & Brew, 1980; Zak et al., 1983; Zak & Aisen, 1985; Mason et al., 1987) or by recombinant DNA technology (Funk et al., 1990) has greatly aided the study of transferrins at the molecular level as well as leading to the novel finding that both halves of the protein are necessary for binding to the transferrin receptor with active uptake of iron by cells (Mason et al., 1987).

The large magnitude of the binding constants of ferric ions to transferrins in the presence of bicarbonate and the very long times required to establish equilibrium have made it difficult to characterize the interactions. Considerable effort has been expended through the years to determine whether the binding of metal ions to the two sites in transferrin is cooperative (Warner & Weber, 1953; Aasa et al., 1963; Aisen & Leibman, 1968). By using electrophoretic techniques which allow resolution of the apo, diferric, and each of the two monoferric forms, a slight negative cooperativity was found (Aisen et al., 1978) between the two sites of human transferrin at both pH 6.7 and pH 7.4. Also using electrophoretic methods, Chasteen and Williams (1981) later reported no cooperativity at pH 7.0–7.5 for human transferrin, but mild negative cooperativity at more acid pH and mild positive cooperativity at more basic pH. Williams et al. (1978) reported positive cooperativity for ovotransferrin at pH 5.5 but no cooperativity at pH 6.0. Kinetics of iron release from serum transferrin have also been analyzed in terms of site interactions (Baldwin, 1980). Al-

† This study was supported by grants from the National Institutes of Health to J.F.B. (GM-42636) and to R.C.W. (DK-21739).

* Address correspondence to this author.

‡ University of Massachusetts.

§ University of Vermont.

0006-2960/91/0430-11660$02.50/0

though the quantitation of site interactions requires more study, it would appear from these results that some communication between sites can occur.

The present calorimetric study focuses on the binding of ferric ions, chelated with nitrilotriacetate (NTA),[1] to the two sites in ovotransferrin (OTF). Important distinctions are made between two discrete processes which can be separated on the time axis: the fast, relatively labile binding of Fe-NTA, where NTA acts as an inefficient synergistic anion (Bates & Wernicke, 1971; Woodworth et al., 1975), followed by kinetic trapping of the initially bound iron when bicarbonate replaces NTA in a slower process. It is shown that the strong preference of ferric ion for the N site over the C site is established from the combined effects of the thermodynamics of the fast step and the kinetics of the slow step while the thermodynamics of the overall process play no role.

Linkage between sites, when it occurs, must be expressed through ligand-dependent changes in domain–domain interactions. Using half-molecules OTF/2C and OTF/2N, these interactions are studied directly by titration calorimetry, and the results allow estimates of the changes in domain interactions as these depend on iron binding to either or both sites.

Materials and Methods

Ovotransferrin (OTF, apo form, from chicken egg white; catalogue no. C-0755, lot 107F-8020) and nitrilotriacetate (NTA, catalogue no. N-0253, lot 37F-0669) were from Sigma Chemical Co. and used without further purification. All other chemicals were reagent grade.

Solutions of the chelated ferric ion (Fe-NTA) were prepared by mixing 1 volume of 0.5 M $FeCl_3$ (in 0.05 M HCl) with 2 volumes of 0.5 M NTA in water and then diluted to the appropriate concentration with 0.10 M HEPES buffer solution (with or without 0.025 M $NaHCO_3$), pH 7.5. The pH was readjusted to 7.5 using a small amount of concentrated NaOH solution. All buffer solutions were treated with a chelating resin to minimize heavy-metal ions.

The N- and C-terminal half-molecules, OTF/2N and OTF/2C, were prepared using the method of Oe et al. (1988), with minor modifications, from ovotransferrin prepared according to Brown-Mason and Woodworth (1984). All protein solutions were exhaustively dialyzed against buffer solutions prior to carrying out calorimetric studies. Preliminary estimates of concentration for apo forms were determined spectrophotometrically at 280 nm using an extinction coefficient of 92000 (apo-OTF), 44000 (apo-OTF/2C), and 51000 (apo-OTF/2N) M^{-1} cm^{-1}. However, final concentrations used in data analysis were determined by spectrophotometric titration with Fe-NTA, assuming one ferric ion bound per mole of apo fragment and two per mole of apo-OTF. Concentrations of the ferric forms of the fragments were determined spectrophotometrically at 465 nm using extinction coefficients of 2300 (Fe-OTF/2N) and 2500 M^{-1} cm^{-1} (Fe-OTF/2C).

For titrations to be carried out in the presence of bicarbonate, the bicarbonate was added immediately before carrying out the experiment. For titrations in the absence of bicarbonate, the solutions or buffers were stored overnight with stirring in a vacuum desiccator containing soda lime. Immediately before the experiment, the calorimeter cell and injection syringe were purged with argon and the solutions added directly from the desiccator.

[1] Abbreviations: OTF, hen ovotransferrin; NTA, nitrilotriacetate; OTF/2N and OTF/2C, half-molecule fragments of OTF; Fe-NTA, solution consisting of Fe^{+3} and NTA in a 1:2 molar ratio.

Titration Calorimetry. The titration of apo-OTF and its fragments with Fe-NTA and the reassociation of N and C half-molecules were carried out on a MicroCal OMEGA ultrasensitive titration calorimeter (MicroCal Inc., Northampton, MA) using the Origin software supplied with the instrument. The instrument, software, and data analysis have been described elsewhere (Wiseman et al., 1989). Data points were collected every 2 s in most cases, with no subsequent filtering. Although the software provides automatic determination of the resting base line before integration, it was found that manual peak-by-peak determination of base line resulted in integrated data with less scatter in most cases so that procedure was used. The plotted data curves shown in the figures in this paper are after subtraction of the resting base line that was used for integration purposes.

The mathematical model for two independent sets of sites, used for curve fitting, is described in the Appendix. During fitting of the integrated data to obtain best values of binding parameters, it is possible to float all parameters or to select some parameters to be fixed and others to be floated during iterations. Parameters chosen to be "fixed" can be assigned a numerical value or can be assigned a value determined by other floating parameters (e.g., the stoichiometric parameter n_1 can be fixed by a mathematical equation relating its value to the value of n_2, which is being floated). In this study, all parameters were floated except in those cases noted in the text. Other details for each type of experiment are provided below:

Reassociation Experiments. For each binding isotherm, 14–18 automatic injections were made from a 150-μL injection syringe containing a solution of one of the half-molecules (ca. 0.3 mM) into the reaction cell (1.4 mL) containing the other half-molecule at a 15–20-fold lower concentration. The volumes delivered were identical (8–10 μL delivered over a 15-s duration) for each injection within a set and spaced at 4-min intervals to allow complete equilibration between injections. Control runs were carried out identically, except with no protein in the reaction cell.

Fe-NTA Binding Experiments. The 150-μL injection syringe was loaded with Fe-NTA solution (2-fold molar excess of NTA) at a concentration 20–30-fold higher than the concentration of protein binding sites in the solution contained in the reaction cell. A series of automatic injections of 4–10 μL each was carried out, with 4–30 min between each injection, depending on the kinetics of the binding reactions at the various temperatures. Control experiments were carried out identically except omitting the protein from the reaction cell.

Results

Binding of Fe^{+3}. (A) Native OTF in the Presence of Bicarbonate. Figure 1A shows raw data (27 °C) from the calorimetric titration of 1.4 mL of 0.038 mM apo-OTF (100 mM HEPES, pH 7.5, and 25 mM $NaHCO_3$) with a ligand solution containing 1.56 mM ferric ion (chelated with a 2:1 molar excess of NTA) in the same buffer. There are 15 equivalent 5-μL injections (spaced at 8-min intervals) of ligand solution into protein solution shown in the sample data, while the control experiment has 20 5-μL injections (spaced at 4-min intervals) of identical ligand solution into the same buffer but without protein. It is known that Fe-NTA exhibits a strong preference for the N site (Williams et al., 1978), so it is evidence that injections 1–5 lead to binding primarily at that site. Likewise, injections 7–11 are primarily concerned with saturating the C site. Injections 13–15 are very similar to the control injections and merely represent the rather large endothermic heat of dilution of ligand after saturation of both sites has taken place.

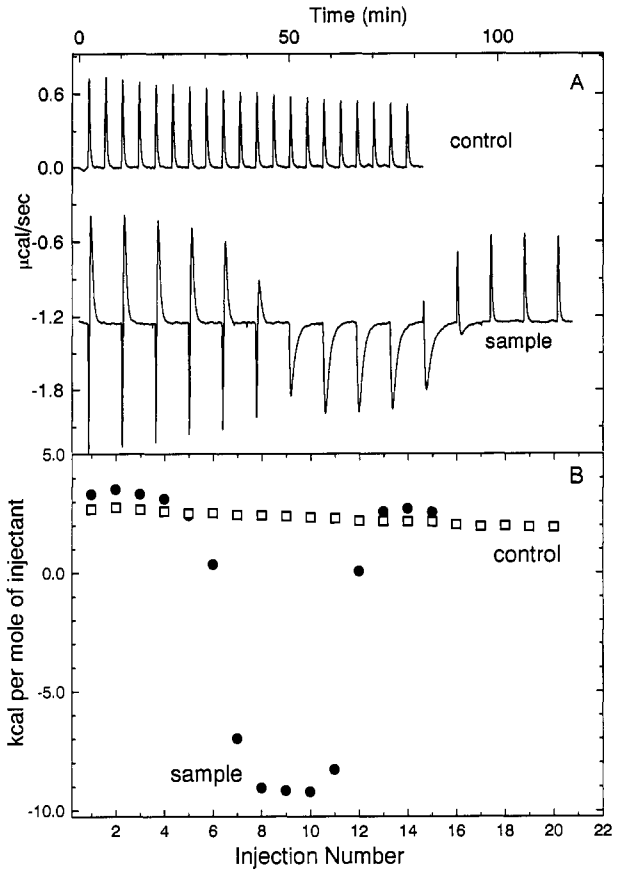

FIGURE 1: Results from titration calorimetry on the binding of Fe-NTA to OTF in the presence of 25 mM bicarbonate, pH 7.5 at 27 °C. Figure 1A shows the raw data for 15 injections, 5 μL each, of 1.56 mM Fe-NTA into the 1.4-mL containing 0.038 mM apo-OTF. The 20 control injections were carried out in the same way except with no OTF in the cell. Figure 1B shows the integrated areas for each of the sample and control injections, expressed in terms of kilocalories per mole of ligand injected.

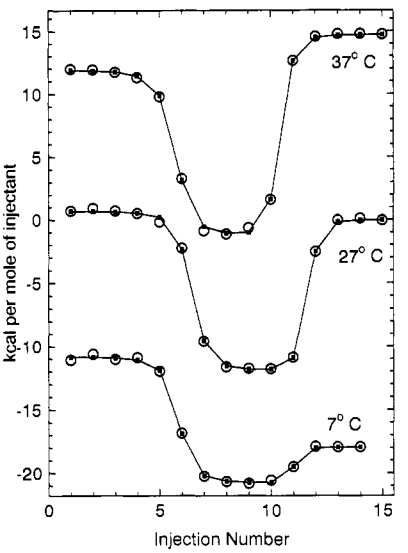

FIGURE 2: Integrated areas for the titration of OTF with Fe-NTA at temperatures of 7, 27, and 37 °C in the presence of 25 mM bicarbonate, after subtraction of controls. Solution conditions are as in Figure 1. The open circles are the experimental heats for each injection, while the solid squares are the calculated values using the binding parameters shown in Table I. The curves for data at 37 and 7 °C have been arbitrarily shifted on the ordinate scale to avoid overlap of data points.

Table I: Thermodynamic Constants for Binding of Fe-NTA to Native OTF, in the Presence of 25 mM Bicarbonate, pH 7.5

		site 1		site 2	
temp (°C)	K_1/K_2	ΔH_1 (kcal)	ΔC_{p_1} (cal/deg)	ΔH_2 (kcal)	ΔC_{p_2} (cal/deg)
7.0	320	7.20	−335	−2.9	−440
27.0	340	0.75	−335	−12.1	−440
37.0	215	−2.80	−335	−16.2	−440

There are two kinetic phases associated with binding Fe-NTA at the N site, evident in the first five injections. Immediately following injection, there is an initial exothermic phase (which we will refer to as *contact binding*) which is faster than the response of the instrument. This is followed by a slower endothermic phase which lasts for ca. 3 min at this temperature. For the C site, contact binding is also exothermic, but it is not seen as a separate peak at this temperature since it is almost exactly canceled out by the endothermic heat of dilution. The slow phase for the C site is exothermic, in contrast to the N site, and noticeably slower.

The total integrated heats associated with each sample injection are shown in Figure 1B along with the corresponding values for the control injections. Note that the control heats become slightly smaller with successive injections. As might be expected, the last three injections in the sample series (i.e., after saturation of both sites) agree more closely with the first three injections in the control series (which have nearly the *same concentration of free ligand*) rather than with the numerically corresponding injections (which have the *same bulk concentration of ferric ion*). Consequently, each sample injection was corrected by subtracting a constant value for the heat of dilution, that being the average of the last three injections in the sample series.

Identical experiments to those described above at 27 °C were also carried out at both higher and lower temperatures of 37 and 7 °C. As the temperature is raised, the heat changes for both the fast and slow phases for each site become more exothermic and the kinetics for the slow phases become faster (ca. 3–4 times faster at 37 °C than at 7 °C). The final integrated heats (after subtraction of the heat of dilution in the manner indicated above) at each temperature are shown as open circles in Figure 2, where the top and bottom curves have been displaced for clarity. All three data sets show the same qualitative pattern since injections 1–4 show a constant heat of binding, followed by a sharp dropoff at 50% saturation to a new heat of binding which then remains constant for injections 7–11 until 100% saturation. It is clear from this that the sites titrate in nearly a sequential fashion, with the C sites beginning to titrate appreciably only after the N sites are virtually saturated. If cooperativity between sites exists, then it does not act to overcome the strong preference for the N site. Using a Marquardt alogrithm (see Appendix) based on two independent binding sites in OTF, we attempted to deconvolute the data to obtain binding parameters, which are shown in Table I. It was found that absolute values of the *apparent* binding constants K_1 and K_2 were not well-defined by the data, as expected since they are very large, but that highly accurate estimates of the heats of binding, ΔH_1 and ΔH_2, and at least crude estimates of the ratio of apparent binding constants, K_1/K_2, could be obtained. The fitting results (small closed squares) are also shown in Figure 2. During the fitting, the stoichiometry parameters for each site, n_1 and n_2, were also floated with final values between 0.95 and 1.05 in all cases.

The results in Table I confirm the strong preference for the first ferric ion to bind to the N site with K_1/K_2 values in excess of 200 at all three temperatures. Since binding to the C site

is more exothermic at all temperatures by more than 10 kcal (e.g., −16.2 vs −2.8 kcal/mol for the N site at 37 °C), the strong preference for the N site would require it to have a more positive ΔS of binding of at least 50 eu *if it is assumed that binding is thermodynamically controlled.* As will be shown later, this is probably not the case in the presence of bicarbonate, and the ratio K_1/K_2 is merely a representation of site preference which is controlled by kinetic as well as thermodynamic factors.

The temperature dependence of ΔH reveals both sites have a large negative ΔC_p of binding, with estimates of −335 and −440 cal/deg for the N and C sites, respectively, determined as an average value over the range from 7 to 37 °C. Negative heat capacity changes are often associated with the burial of hydrophobic side chains, as first shown many years ago (Brandts, 1964). If that is the correct explanation here, it may indicate that conformational changes in the direction of a more compact structure accompany the binding of ferric ion to each site.

The ΔH and ΔC_p values in Table I represent the total for both the fast and slow phases of Fe-NTA binding. Because of overlap on the time axis, it is only possible to make approximate estimates for each phase individually. For example, at 27 °C, we estimate that contact binding has a ΔH of −6.5 kcal for the N site and −3 kcal for the C site while the respective values for the slow phases are +7 and −9 kcal. It is also clear that there are contributions to the total ΔC_p from both the fast and slow phases for each site.

If protons are released during the binding process, then they will bind to the buffer and the heat of protonation will also be included in the data in Table I. In order to estimate this effect, some experiments were carried out in Tris buffer, which has a larger heat of ionization than HEPES (11.30 vs 3.92) by 7.38 kcal/mol at 25 °C (Grime, 1985). At 27 °C in the presence of 25 mM bicarbonate, it was found that the total heat for binding Fe-NTA to the N site was more negative in Tris buffer by −3.7 kcal and that binding to the C site was more negative by −3.5 kcal. This suggests that 0.5 proton is released when Fe-NTA binds to either of the two sites at 27 °C, so that ΔH_1 and ΔH_2 values in Table I would be ca. 2 kcal more positive after correcting for proton release. Earlier pH titrations of OTF (Warner & Weber, 1953) and human transferrin (Aasa et al., 1963) indicated a release of slightly less than 3.0 per site, when iron was added as a $FeCl_3$ solution into an unbuffered protein solution at pH 7.5. Our results would be in accord with theirs if it is assumed that NTA picks up ca. two protons after it is released from chelation with Fe^{+3}.

Earlier calorimetric studies (Binford & Foster, 1974) reported on the binding of Fe-NTA to human serum transferrin in Tris buffer at pH 7.96, 25 °C. They found experimentally identical ΔH values for binding to the first and second sites, with values of ca. −11 kcal in the presence and −4.5 kcal in the absence of bicarbonate. These results contrast with those on OTF, where large differences are seen in ΔH for the two sites.

(B) Native OTF in the Absence of Bicarbonate. Both fast and slow phases in the binding of Fe-NTA to serum transferrin have previously been observed (Bates & Wernicke, 1971) by stopped-flow spectrophotometry. The fast phase was attributed to rapid binding of the chelated ferric ion while the slow phase was suggested to involve the replacement of the chelator NTA by bicarbonate ion. This explanation appears to account nicely for our results with OTF. We observed that as the bicarbonate concentration was lowered below 25 mM, the concentration used for the data in Figure 1, the slow phase for both the N and C site becomes slower in nearly inverse proportion to the concentration. If precautions are taken to completely mimimize bicarbonate (see Materials and Methods), then the slow phase cannot be seen at all as shown in the data of Figure 3A at 27 °C. Here, the 25 injections are spaced at 4-min intervals, and it can be seen that complete equilibration requires only ca. 2 min, which is characteristic of other "instantaneous" reactions we have studied. As will become evident below, there are strong similarities between the total binding process shown here in the absence of bicarbonate with the contact binding process in the presence of bicarbonate (cf. Figure 1A). This implies that the slow phase is due to insertion of bicarbonate (with concomitant release of NTA) *after* the ferric ion has already bound to OTF.

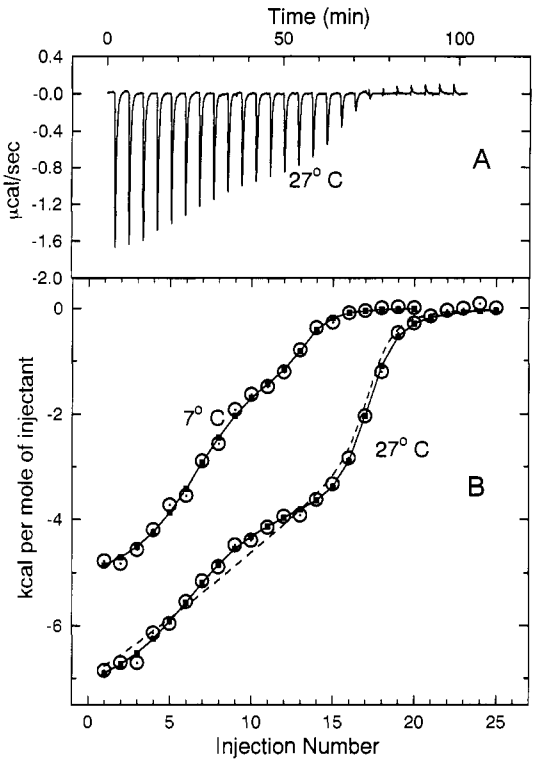

FIGURE 3: Calorimetric titration of OTF with Fe-NTA in the absence of bicarbonate at 7 and 27 °C, pH 7.5. Figure 3A shows the raw data for 25 injections at 27 °C, while Figure 3B shows integrated data (open circles) at both 7 and 27 °C, after subtraction of controls. The solid lines pass through the corresponding calculated points obtained using the binding parameters in Table II. The dashed curve for the data at 27 °C represents the best fit of the data using the constraint $n_1 = n_2$.

Experiments carried out at 7 °C (not shown) in the absence of bicarbonate were generally similar to those at 27 °C and support the same conclusion. At the lower temperature, however, there was the vestige of a "slow" endothermic phase after the fast exothermic binding at the N site, but it was less than 10% of the size of the equivalent slow peak seen in the presence of bicarbonate and was much faster. Although various interpretations are possible, this could result from insertion of a weak binding HEPES anion after contact binding of Fe-NTA, since many other anions are known to bind to holotransferrins in the absence of bicarbonate (Harris & Aisen, 1989).

The total integrated heats for each injection at both 7 and 27 °C are shown in Figure 3B, after subtraction of the small dilution control. These data show that although there is still a preference for the first ferric ion to bind to the more exothermic N site in the early injections, this preference is weaker than when bicarbonate is present. Consequently, there is a

Table II: Best Values for Fitting Parameters for Binding Fe-NTA to Native OTF, in the Absence of Bicarbonate, pH 7.5

	site 1			site 2		
temp (°C)	n	ΔH (kcal)	$K \times 10^{-6}$	n	ΔH (kcal)	$K \times 10^{-6}$
7	0.94	−5.36	21	1.03	−0.84	2.1
27	0.71	−7.60	25	1.28	−3.60	2.3

more gradual change in the heat signal near the point of 50% saturation (i.e., between injections 7 and 8 at 7 °C and between 10 and 11 at 27 °C), in contrast to the very abrupt changes seen in Figure 2.

The data in Figure 3B were deconvoluted assuming a model with two independent sites, and the final fitting results are shown as the solid line with the best-fit parameters in Table II. The data taken at 7 °C are described reasonably well by the fit curve with best values for parameters (n_i, ΔH_i, K_i) of 0.94, −5.36 kcal, and 2.1×10^7, respectively, for the N site and 1.03, −0.84 kcal, and 2.1×10^6, respectively, for the C site. These results suggest that the N site is only ca. 10 times stronger than the C site in the absence of bicarbonate, in contrast to K_1/K_2 ratios of several hundred in its presence. Paradoxically, a good fit of the data at 27 °C could not be obtained using nearly equal n_1 and n_2 values. The dashed line represents the best fit using the constraint $n_1 = n_2$. The fit shown as the solid line was the best fit with no constraints and leads to parameters 0.71, −7.6 kcal, and 2.5×10^7 for the N site and 1.28, −3.6 kcal, and 2.3×10^6 for the C site, i.e., n_2 is over 50% larger than n_1. These experiments at 7 and 27 °C were each repeated 2 more times, with the same results. Since it is certain that n_1 and n_2 must in fact be equal, the difficulty probably arises because the model of two independent sites is inappropriate.[2] This would occur for example if the K and/or ΔH values for binding to each site depended on whether the other site was filled or vacant. To properly deconvolute such data would require a model based on *two nonidentical, interacting sites*. However, such a model requires 10 fitting parameters, including n_1 and n_2, which is more than can be uniquely determined from most binding data, including these. There is no intention here to imply that it is the absence of bicarbonate ion which leads to site–site interaction in OTF. In fact, the model of two nonidentical, interacting sites becomes completely equivalent to the model of two nonidentical, independent sites whenever one site is intrinsically much stronger than the other (i.e., the progress of saturation will be unaffected whenever site–site interactions are much smaller than the intrinsic difference between the two sites). Thus, the good fit of the model of independent sites in the presence of bicarbonate could result from the fact that the apparent K values are different by a factor of several hundred, whereas they become more similar in the absence of bicarbonate which then reveals the true interacting nature of the sites. Likewise, the better fit of the model of independent sites to the data obtained in the absence of bicarbonate at 7 °C relative to the obviously poor fit at 27 °C could also result from K values being closer in magnitude at the higher temperature, in view of the substantially larger negative ΔH value for the N site in the absence of bicarbonate. Evidence presented below on the interaction of N and C fragments with one another confirms that the two sites in OTF are not independent of one another, even in the presence of bicarbonate.

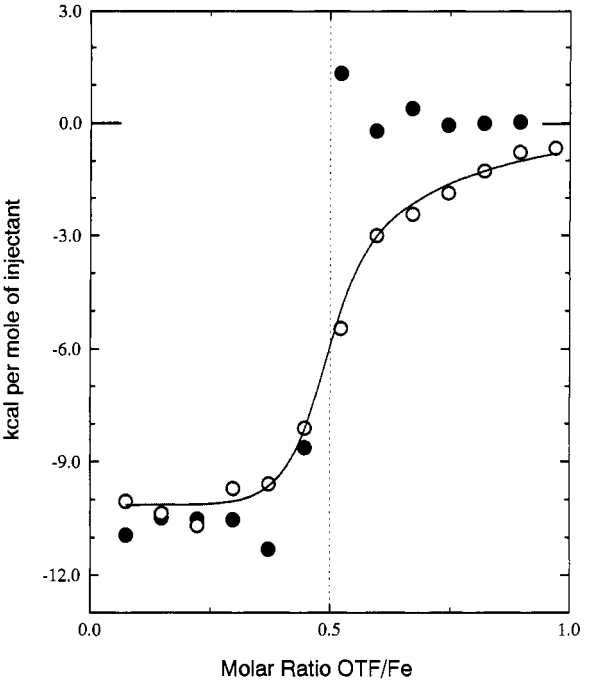

FIGURE 4: Reverse titrations where Fe-NTA solution is initially in the sample cell and OTF solution in the injection syringe, at 27 °C. Other conditions as in Figure 1. The filled circles were obtained in the presence of 25 mM bicarbonate while the open circles were obtained in the absence of bicarbonate.

Although the estimates of individual ΔH values (i.e., −7.7 and −3.6 kcal at 27 °C) in Table II must be treated as approximate (the sum of the two should be quantitative) in view of the inexact nature of the model used to fit the data, they do agree well with our earlier estimates of ΔH (−7 and −4 kcal at 27 °C) for just the fast phases in the presence of bicarbonate.

(*C*) *Reversibility of Binding.* Early in this project, we carried out some studies using the avid iron scavenger deferrioxamine mesylate. We discovered that this scavenger was able to extract ferric ions from OTF immediately after contact binding occurred but was no longer able to extract efficiently after the slow replacement of NTA with bicarbonate had taken place. This suggested the possibility that exchange of ferric ions between N and C sites might not take place freely during the time span of titrations. In order to demonstrate limitations in reversibility under the conditions used in this study, we have carried out two titrations (27 °C) in the reverse direction (i.e., progressing from low to high protein:ligand ratios rather than from high to low) from those discussed above. In this case, the apo-OTF solution was loaded into the syringe and then injected into a solution containing Fe-NTA in the cell. Since Fe-NTA will be in excess, the early injections will saturate both the N and C sites of OTF, and the heat change will be $\Delta H_1 + \Delta H_2$. With further injections, all of the Fe^{+3} will be bound as diferric OTF when the molar ratio of OTF to Fe-NTA is 0.5. As more OTF is added, then some of the Fe-NTA which is bound to the weaker site of diferric OTF will detach and bind to the stronger site of the apo-OTF which is added,

[2] In searching for other explanations for the poor fit of these data at 27 °C to the model, it occurred to us that the variable concentration of free NTA in the reaction cell could be a problem. That is, in the experiments illustrated in Figure 3, the initial concentration of free NTA in the reaction cell was zero, and this increased with each injection of Fe-NTA after ferric ions bind and the excess NTA goes into solution. To check on this, several other experiments were carried out in the same manner except that a substantial amount of NTA (up to 4 times the concentration of binding sites) was added to the transferrin solution before injections of Fe-NTA were started. This ensured that there would only be a small percentage change in the free NTA concentration throughout the series of injections. Although this led to slightly smaller apparent binding constants at both sites, the data showed exactly the same kinds of problems when fitting with a model of independent sites.

if it is assumed that the binding is reversible. The heat change for this second phase of the titration will be the difference between ΔH_1 and ΔH_2. When sufficient OTF has has been added to form entirely monoferric OTF, then the heat signal will go to zero with further injections.

Results from these reverse titrations are shown in Figure 4 both in the presence (solid circles) and in the absence (open circles) of 25 mM bicarbonate. In the absence of bicarbonate, it is clear that diferric OTF is formed below 0.5 molar ratio of OTF/Fe and this is converted to monoferric OTF at ratios above 0.5. Although these data are not precise enough to define unique binding parameters nor to observe deviations from the model of independent sites, they do support the idea that binding of Fe-NTA occurs reversibly in the absence of bicarbonate. The solid line shown in Figure 4 for this reverse titration was calculated using ΔH values for sites 1 and 2 which were within 1 kcal of those obtained from titration in the forward direction (cf. Table II) and using K values differing by less than 50% from those obtained in the forward titration.

In the presence of bicarbonate, $\Delta H_1 + \Delta H_2$ should also be −11 kcal while $\Delta H_1 - \Delta H_2$ is +13 kcal, from the data obtained in the forward direction (Table I). Up to molar ratio 0.5, everything is as expected (Figure 4, solid circles) for the formation of 100% diferric OTF with heats near −11 kcal/mol. At ratios higher than 0.5, there is no evidence (the seventh injection does show a slight positive value, but this is due to the fact that there is a small amount of ferric ion still unbound after the sixth injection, so this binds preferentially to the N site during the next injection as expected) that ferric ion initially bound to the weaker site of diferric OTF is able to dissociate and migrate to the stronger site of the excess apo-OTF which is injected. If this were occurring, then the heat would rise to +13 kcal/mol, rather than remaining at zero, if it is assumed that the N site is the stronger.

We conclude from these results that binding in the absence of bicarbonate or contact binding in the presence of bicarbonate is reversible or nearly reversible within our time frame and an equilibrium is set up in accordance with the binding constants which exist *at that time.* On the other hand, the distribution of ligands between N and C sites becomes largely frozen once the slow phase has taken place and bicarbonate ion has entered the binding pocket. Even though the free concentration of chelator NTA is as high as 0.1 mM toward the end of the titration in the presence of bicarbonate, ferric ions are still unable to migrate from the weaker to the stronger site within our time frame. This means the final distribution of ligands is influenced more by the contact binding constants than by the final binding constants and that the relative kinetics of the essentially irreversible slow phase for the N and C site will also make a significant contribution to the final ligand distribution.

(D) Binding to Fragments OTF/2N and OTF/2C. There is the indication of site–site interaction in the data presented above which means that the properties of native OTF should be more than merely the sum of properties of the two half-molecules. The four curves in Figure 5 show raw data from a single injection of Fe-NTA at 27 °C in the presence of 25 mM bicarbonate. At the qualitative level, the response of the C fragment to iron binding is extremely similar to the corresponding response seen for binding to the C site in intact OTF. The same is true in the comparison of binding to the N fragment and binding to the N site in intact OTF. In the analysis of total binding isotherms based on many injections, some quantitative differences do show up in the heats of binding shown for both fragments in Table III. For comparison, the values obtained earlier for the N and C sites in intact OTF are shown in parentheses. The heat of binding Fe-NTA to the N fragment is more positive than for binding to the N site in intact OTF by 3 kcal at 7 °C and by 1.25 kcal at 27 °C. Likewise, the heat of binding to the C fragment is also more positive by ca. 3 kcal at both 7 and 27 °C, relative to the C site in OTF. It will be shown that this trend for binding of Fe-NTA to occur more exothermically to OTF than to the fragments results from ligand-dependent changes in interactions between the two domains in OTF.

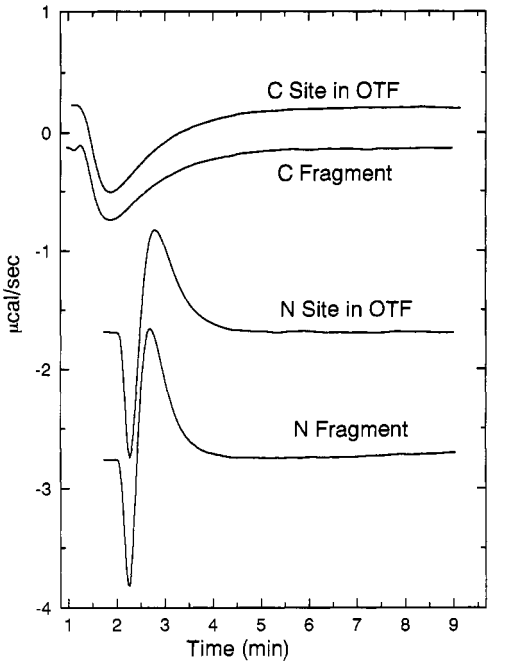

FIGURE 5: Raw data from a single injection of Fe-NTA at 27 °C, corresponding to (top to bottom) binding to the C site in OTF, the C fragment OTF/2C, the N site in OTF, and the N fragment OTF/2N.

Table III: Estimates of ΔH for Binding Fe-NTA to OTF/2N and OTF/2C Fragments in 25 mM Bicarbonate, pH 7.5[a]

temp (°C)	OTF/2N ΔH (kcal)	OTF/2C ΔH (kcal)
7	10.2 (7.2)	0.4 (−2.9)
27	2.0 (0.75)	−9.5 (−12.1)

[a] Values in parentheses are for the same site in intact OTF.

Titrations of both the C fragment and the N fragment were also carried out in the absence of bicarbonate ion at 27 °C, and as with intact OTF, no slow phases were seen. The heats of injection are shown in Figure 6, along with the fit curves and fitting parameters. As expected from the studies on intact OTF in the absence of bicarbonate, the ΔH of binding to the N site (−12.9 kcal) is considerably more exothermic that for binding to the C site (−2.7 kcal). The binding constant to the N fragment is ca. 5 times larger than to the C fragment. Under similar conditions for intact OTF, the indicated binding constants were both somewhat higher and their ratio was 10 rather than 5, but those results are less certain due to problems in fitting the data to a model of independent sites.

Binding of OTF/2N to OTF/2C. If saturating amounts of Fe-NTA are added to either half-molecule in the presence of bicarbonate and the excess ligand and chelator dialyzed away, the attached ferric ion is bound irreversibly for all practical purposes. It is then possible, for example, to study the direct binding of the apo form of OTF/2N to the ferric form of OTF/2C without the danger of the ferric ion migrating from the C fragment to the N fragment after mixing. Using this

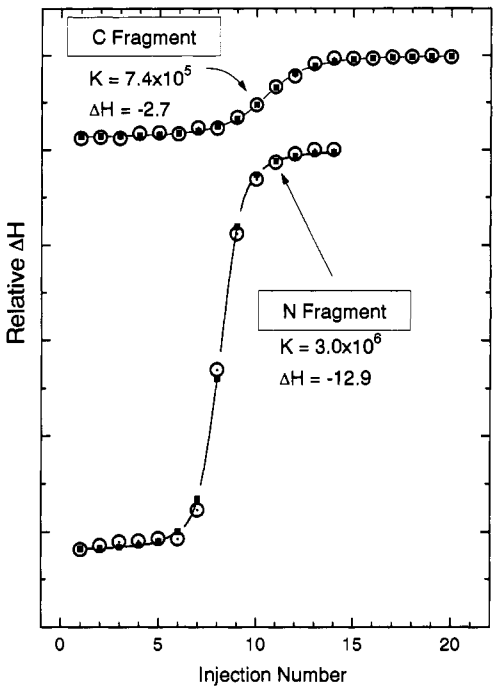

FIGURE 6: Integrated data (open circles) for the binding of Fe-NTA to OTF/2C (upper curve) and OTF/2N. The solid squares show the calculated values from the best-fit analysis, using the indicated binding parameters.

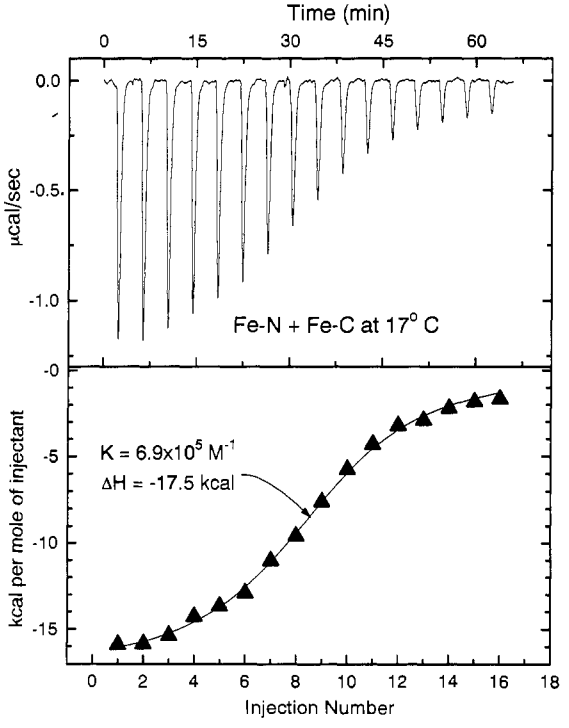

FIGURE 7: Titration of the ferric form of OTF/2N (0.021 mM) with 16 8-μL injections of the ferric form of OTF/2C (0.343 mM) at 17 °C, pH 7.5. The raw data are shown in the upper frame and the integrated heats in the lower frame, after subtraction of the control heats. The best-fit line is shown in the lower frame, along with the binding parameters obtained from the fit.

approach, we have studied the four pairwise permutations of interaction between the two fragments at three temperatures of 6, 17, and 27 °C. One data set is shown in Figure 7 for the interaction between the ferric forms of the two fragments at 17 °C. The raw data, consisting of 16 identical injections spaced at 4-min intervals, are shown in the upper panel. The interaction is characterized by exothermic heat effects with

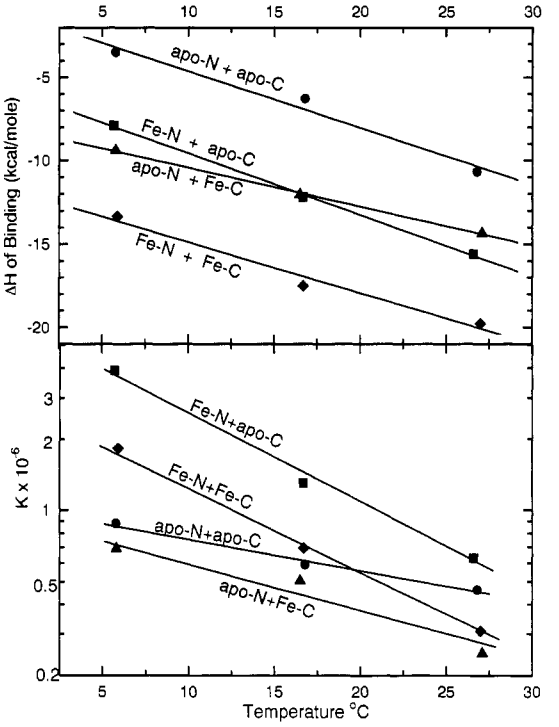

FIGURE 8: Heats of binding (upper) and binding constants (lower) for the interaction of fragments OTF/2C and OTF/2N, in the presence and absence of site saturation.

no indication of slow kinetics. This was observed to be true of all four pairwise permutations at each of the three temperatures. The integrated heats are shown in the lower panel, along with the best-fit line obtained from iterative fitting using a model based on a single set of sites (Wiseman et al., 1989). The indicated heat change is −17.5 kcal, and the best value of the binding constant is 6.9×10^5 M^{-1}.

The value of parameters obtained from curve fitting at each temperature are shown in Figure 8. As seen in the upper panel, the heats are largest for interaction of the two ferric forms and smallest for the two apo forms. In all cases, the heats show a strong temperature dependence with an indicated ΔC_p of ca. −350 cal/deg for all pairwise interactions except that between the apo–N and Fe–C fragments which is −200 cal/deg. Again, these large changes in heat capacity are consistent with removal of hydrophobic groups from contact with water upon complexation of the fragments.

Rather surprisingly, the interaction constants (lower panel of Figure 8) do not follow the same trend seen for the heat effects since it is the Fe–N and apo–C combination which shows the strongest interaction at all temperatures while the apo–N and Fe–C combination is the weakest. In fact, tighter interactions occur in both cases where a ferric ion is added to the N site of an interacting pair (i.e., apo–N/apo–C going to Fe–N/apo–C and apo–N/Fe–C going to Fe–N/Fe–C) while weaker interactions occur in both cases where a ferric ion binds to the C site of an interacting pair.

If the two iron binding sites were independent in the complexes formed between OTF/2N and OTF/2C, then all of the K and ΔH values for the four pairs in Figure 8 would be the same at each temperature. Since K values differ by up to a factor of 10 and ΔH values by a factor of 4, it is clear that there is site–site communication and this likely also applies to the two sites in intact OTF. This is in agreement with our earlier observation that data from titration of OTF by Fe-NTA in the absence of bicarbonate could not be fit well by a model of independent sites. It will be shown under Discussion that

variations in fragment interactions as a function of site saturation, and analogous variations in domain interactions in intact OTF, must necessarily produce a counterpart effect on the corresponding binding constants for ferric ions if thermodynamic control is assumed.

Discussion

Our results show that there are two kinetic processes associated with the binding of Fe-NTA to OTF in the presence of bicarbonate. Contact binding is very fast while the insertion of a bicarbonate ion to replace NTA occurs on a time scale of minutes under our conditions. Contact binding is exothermic at both sites, more so at the N site, while bicarbonate insertion is endothermic at the N site and exothermic at the C site over most of the temperature range of our investigation. There are large negative ΔC_p values for binding of Fe-NTA at each of the sites, which leads to a strong temperature dependence of ΔH and suggests that binding of ferric ions tightens the protein structure and removes hydrophobic groups from contact with water. Along these lines, the crystal structure of lactoferrin (Anderson et al., 1989) shows the binding site in each domain is buried ca. 10 Å below the surface in a pocket which appears large enough to accommodate some solvent molecules. It has been speculated (Harris & Aisen, 1989) that there may be some hinge-type movement of half-lobes within a domain to reduce or increase the size of the pocket as the ligand binds or releases. More recent crystallographic data (Anderson et al., 1990) on lactoferrin show these effects to be particularly large for the N site, since the two half-lobes which form the binding sites are swung rather far apart in the apo form but collapse together to surround the ligand in the ferric form.

It has often been assumed (Harris & Aisen, 1989) that binding of ferric ions to transferrins is controlled by kinetic factors in the absence of chelators (i.e., ferric ions "stick" to the first site which they contact and are then unable to migrate) but thermodynamic factors become more important in the presence of chelators. At our concentrations of NTA and over the relatively short time frame of observation, the situation is more complicated. The initial process of contact binding was demonstrated to be labile and perhaps fully reversible, so that the distribution of ferric ions between the two sites might be quickly established in accordance with the binding constants existing *at that time*. However, once the bicarbonate ion has inserted during the slow phase, then ferric ions are no longer free to migrate between sites. The final distribution of ferric ions between the two sites in the presence of bicarbonate is then not a good indicator of the final binding constants.

Our results show that the K value for Fe-NTA binding to the fragment OTF/2N is only about 4 times larger than to the fragment OTF/2C in the absence of bicarbonate while the ratio could be 10 or larger in intact OTF (there is uncertainty here due to the poor fit using a model based on independent sites) with no bicarbonate present. On the other hand, the *apparent* binding constants to OTF in the presence of bicarbonate are in the ratio of 200 or more. It seems likely that this high ratio reflects two factors: first, there is a strong preference for reversible contact binding to favor the N site; and second, the slow phase for bicarbonate insertion into the N site is significantly faster than for insertion into the C site so the irreversible factors also act to additionally favor the N site.

The two binding sites in transferrins are separated by about 40 Å (Anderson et al., 1989). The question has often been posed as to whether any communication or signaling can occur between these distant sites and, if so, what role this might play in the coordination of ligand binding and the physiological function of these proteins. That such ligand-dependent signaling does occur was verified by studying the direct interactions between the OTF/2N and OTF/2C fragments. It was found that both the interaction constants and the heats of interaction of the fragments with one another are quite dependent not only on how many ferric ions are attached to the interacting pair but also, in the case where only one ferric ion was involved, to which particular site it is attached. The possible significance of this can be illustrated by considering two separate but equivalent thermodynamic paths involving the binding of a single ligand (L) to a protein (N), which is also capable of complexing with another protein (C), i.e.:

$$\begin{aligned} N + C &\rightleftharpoons C\text{–}N \qquad K_B,\ \Delta H_B \qquad \text{(I)} \\ C\text{–}N + L &\rightleftharpoons C\text{–}NL \qquad K_L,\ \Delta H_L \\ N + L &\rightleftharpoons NL \qquad K_L',\ \Delta H_L' \qquad \text{(II)} \\ NL + C &\rightleftharpoons C\text{–}NL \qquad K_B',\ \Delta H_B' \end{aligned}$$

Since both of these paths describe the same total process (i.e., $N + C + L \rightleftharpoons C\text{–}NL$), then it must be true that

$$K_B'/K_B = K_L/K_L'$$

$$\Delta H_B' - \Delta H_B = \Delta H_L - \Delta H_L'$$

The first equation shows that if the liganded form NL binds more strongly to C than does the unliganded form N, then it necessarily follows that the ligand must bind proportionately more strongly to C–N than it does to N alone. Likewise, any ligand-dependent heat effects seen in the interaction of N and C must have its counterpart in C-dependent heat effects in ligand binding. To complete the analogy with OTF, similar conclusions would apply to a second site if the C protein also had a site for binding of L.

Applying these ideas to the data of Figure 8 and assuming that domain–domain interactions in intact OTF respond similarly to the binding of ferric ions as do fragment–fragment interactions, it becomes clear that the two binding sites in OTF cannot be regarded as independent. In the true thermodynamic sense, ligand-dependent changes in interaction between domains will have their counterpart effect on the binding constants and heats of binding of ferric ions. By changes in domain–domain interactions, signals are sent from one site to report on its state of ligation and are received from the other site, thereby providing at least the opportunity for some coordination between sites. The data at 5 °C, for example, suggest that the binding of iron to the N site should be enhanced (i.e., relative to the hypothetical situation where the domains in OTF have constant interactions, irrespective of the state of ligation with Fe^{+3}) 5-fold by increases in domain interactions while the binding of a second iron to the C site is reduced 2-fold due to a reduction in domain interactions. These numbers apply only to the final binding constants in the presence of bicarbonate, while it is the contact binding constants that were shown to be important in determining site preference in our studies of short time duration. There is no way to determine how much of this effect shows up in the contact binding constants since these cannot be estimated accurately due to the inadequacy of the model of independent sites. It does seems likely, however, that some or all of this effect will be felt in the contact binding constants.

In terms of heat changes, the data in Figure 8 lead to the expectation that ΔH for binding the first iron to the N site and the second iron to the C site will both be more negative by 4–5 kcal due to changes in domain interactions in the prescence of bicarbonate. These predictions compare mod-

erately well with direct measurement of the heats of binding, which showed the N site and C site in OTF to be ca. 3 kcal more exothermic on average than for the corresponding site in the isolated fragment.

In summary, this study provides a clear indication that there is interaction between the two sites in OTF but it is not known if this might play any role in carrying out its function.

Appendix

Model for Two Sets of Independent Sites. It is assumed in the following that a macromolecule M has two sets of sites for binding the same ligand X, each set with its characteristic binding constant (K_1, K_2), molar heat of binding (ΔH_1, ΔH_2), and number of sites of that type (n_1, n_2). The sets are assumed to be independent so the fractional saturation for each type of site (Θ_1, Θ_2) can be used as the progress variable during saturation, and

$$K_1 = \frac{\Theta_1}{(1-\Theta_1)[X]} \quad K_2 = \frac{\Theta_2}{(1-\Theta_2)[X]} \tag{1}$$

$$X_t = [X] + M_t(n_1\Theta_1 + n_2\Theta_2) \tag{2}$$

where X_t and [X] are the bulk and free concentration of ligand, respectively, and M_t is the bulk concentration of macromolecule. Solving eq 1 for Θ_1 and Θ_2 and substituting into eq 2 give

$$X_t = [X] + \frac{n_1M_t[X]K_1}{1+[X]K_1} + \frac{n_2M_t[X]K_2}{1+[X]K_2} \tag{3}$$

Clearing eq 3 of fractions and collecting like terms lead to a cubic equation of the form

$$[X]^3 + p[X]^2 + q[X] + r = 0 \tag{4}$$

where

$$p = \frac{1}{K_1} + \frac{1}{K_2} + (n_1+n_2)M_t - X_t$$

$$q = \left(\frac{n_1}{K_2} + \frac{n_2}{K_1}\right)M_t - \left(\frac{1}{K_1} + \frac{1}{K_2}\right)X_t + \frac{1}{K_1K_2} \tag{5}$$

$$r = -X_t/K_1K_2$$

Equations 4 and 5 can be solved for [X] either in closed form or (as done in the calorimetric software) numerically using Newton's method once the bulk concentrations and fitting parameters n_1, n_2, K_1, and K_2 are assigned. Substitution of [X] into eq 1 then gives the values for both Θ_1 and Θ_2.

The above solution is perfectly general and may now be applied to results from titration calorimetry. The heat content Q of the solution contained within the active volume V_0 of the calorimeter cell will in general be

$$Q = M_tV_0(n_1\Theta_1\Delta H_1 + n_2\Theta_2\Delta H_2) \tag{6}$$

In a series of injections (i = 1, 2, ...) of ligand into the cell containing macromolecule, then eq 6 may be used to calculate the heat content $Q(i)$ of the *solution contained in* V_0 after the ith injection. The experimental observable measured by the calorimeter is the difference in heat $\Delta Q(i)$ between the i and $i-1$ injections. A minor complication arises here since the calorimeter cell is lollipop in shape with the expanded working volume V_0 of the cell communicating to the outside through a thin capillary tube. Since the cell and capillary tube are totally filled with solution, each injection of ligand solution dV_i forces liquid out of V_0 and into the inactive tube after its heat effects are felt. Consequently, the measured heat effect will be

$$\Delta Q(i) = Q(i) + \frac{dV_i}{V_0}\left[\frac{Q(i)+Q(i-1)}{2}\right] - Q(i-1) \tag{7}$$

The middle term in the above equation indicates that the heat content of the displaced volume will be the average of that existing before and after the ith injection. This constitutes a small correction since dV_i/V_0 is typically only ca. 0.003. Small corrections for displaced volumes are also applied in software calculations of M_t and X_t after each injection.

The procedure used for curve-fitting is then as follows. When experimental injection data $\Delta Q_{ex}(i)$ are in memory, initial guesses for the six fitting parameters (n_1, n_2, K_1, K_2, ΔH_1, and ΔH_2) are made automatically (or the operator may intervene with his own guesses). Having numerical values for each fitting parameter as well as X_t and M_t, eq 1–7 may be used to determine calculated values $\Delta Q(i)$ to compare with the corresponding experimental values $\Delta Q_{ex}(i)$ for all values of i. On the basis of the sum of the squared residuals and standard Marquardt methods, the initial guesses for fitting parameters are improved until the point where subsequent iterations show no further improvement in fit, thereupon arriving at the "best values" for all fitting parameters. At any point, the operator may reduce the number of floating variables by assigning numerical constraints (e.g., $n_1 = 1.0$) or variable constraints (e.g., $n_1 = n_2$) to certain parameters.

Registry No. Fe, 7439-89-6; HCO_3^-, 71-52-3.

References

Aasa, R., Malmstrom, B. G., Saltman, P., & Vanngard, T. (1963) *Biochim. Biophys. Acta 75*, 202–223.

Aisen, P., & Leibman, A. (1968) *Biochem. Biophys. Res. Commun. 30*, 407–413.

Aisen, P., Leibman, A., & Zweier, J. (1978) *J. Biol. Chem. 253*, 1930–1937.

Anderson, B. F., Baker, H. M., Norris, G. E., Rice, D. W., & Baker, E. N. (1989) *J. Mol. Biol. 209*, 711–734.

Anderson, B. F., Baker, H. M., Norris, G. E., Rumball, S. V., & Baker, E. N. (1990) *Nature 344*, 784–787.

Bailey, S., Evans, R. W., Garrat, R. C., Gorinsky, B., Hasnaint, S., Horsburgh, C., Jhoti, H., Lindley, P. F., Mydin, A., Sarra, R., & Watson, J. L. (1988) *Biochemistry 27*, 5804–5812.

Baldwin, D. A. (1980) *Biochim. Biophys. Acta 623*, 183–198.

Bartfeld, N. S., & Law, J. H. (1990) *J. Biol. Chem. 265*, 21684–21691.

Bates, G. W., & Wernicke, J. (1971) *J. Biol. Chem. 246*, 3679–3685.

Binford, J. S., Jr., & Foster, J. C. (1974) *J. Biol. Chem. 249*, 407–412.

Brandts, J. F. (1964) *J. Am. Chem. Soc. 86*, 4302–4311.

Brown-Mason, A., & Woodworth, R. C. (1984) *J. Biol. Chem. 259*, 1866–1873.

Chasteen, N. D., & Williams, J. (1981) *Biochem. J. 193*, 717–727.

Chasteen, N. D., & Woodworth, R. C. (1990) in *Iron Transport and Storage* (Ponka, P., Schulman, H. M., & Woodworth, R. C., Eds.) pp 68–79, CRC Press, Boca Raton, FL.

Dubach, J., Gaffney, B. J., More, K., Eaton, G. R., & Eaton, S. S. (1991) *Biophys. J. 59*, 1091–1100.

Funk, W., MacGillivray, R. T. A., Mason, A. B., Brown, S. A., & Woodworth, R. C. (1990) *Biochemistry 29*, 1654–1660.

Grime, J. K. (1985) in *Analytical Solution Calorimetry* (Grime, J. K., Ed.) pp 299-390, Wiley & Sons, New York.
Harris, D. C., & Aisen, P. (1989) in *Iron Carriers and Iron Proteins* (Loehr, T. M., Ed.) pp 239-351, VCH Publishers Inc., New York.
Lineback-Zins, J., & Brew, K. (1980) *J. Biol. Chem. 255*, 708-713.
Mason, A. B., Brown, S. A., Butcher, N. D., & Woodworth, R. C. (1987) *Biochem. J. 245*, 103-109.
Oe, H., Doi, E., & Hirose, M. (1988) *J. Biochem. 108*, 1066-1072.
Schlabach, M. R., & Bates, G. W. (1975) *J. Biol. Chem. 250*, 2182-2188.
Warner, R. C., & Weber, I. (1953) *J. Am. Chem. Soc. 75*, 5094-5101.
Williams, J. (1974) *Biochem. J. 141*, 745-752.
Williams, J., Evans, R. W., & Moreton, K. (1978) *Biochem. J. 173*, 535-542.
Williams, S. C., & Woodworth, R. C. (1973) *J. Biol. Chem. 248*, 5848-5853.
Wiseman, T., Williston, S., Brandts, J. F., & Lin. L.-N. (1989) *Anal. Biochem. 17*, 131-137.
Woodworth, R. C., Virkaitis, L. M., Woodbury, R. G., & Faval, R. A. (1975) in *Proteins of Iron Storage and Transport in Biochemistry and Medicine* (Crichton, R. R., Ed.) pp 39-50, North-Holland Publishing Co., Amsterdam.
Zak, O., & Aisen, P. (1985) *Biochim. Biophys. Acta 829*, 348-353.
Zak, O., Leibman, A., & Aisen, P. (1983) *Biochim. Biophys. Acta 742*, 490-495.

A Totally Synthetic Histidine-2 Ferredoxin: Thermal Stability and Redox Properties†

Eugene T. Smith,‡ John M. Tomich,§ Takeo Iwamoto,§ John H. Richards,∥ Yuan Mao,‡ and Benjamin A. Feinberg*,‡

Department of Chemistry, The University of Wisconsin—Milwaukee, P.O. Box 413, Milwaukee, Wisconsin 53201, Department of Biochemistry, University of Southern California, Childrens Hospital of Los Angeles, P.O. Box 54700, Los Angeles, California 90054-0700, and Division of Chemistry and Chemical Engineering, California Institute of Technology, Pasedena, California 91125

Received May 28, 1991; Revised Manuscript Received September 10, 1991

ABSTRACT: The entire polypeptide of *Clostridium pasteurianum* ferredoxin (Fd) with a site-substituted tyrosine-2 → histidine-2 was synthesized using standard *t*-Boc procedures, reconstituted to the 2[4Fe-4S] holoprotein, and compared to synthetic *C. pasteurianum* and native Fds. Although histidine-2 is commonly found in thermostable clostridial Fds, the histidine-2 substitution into synthetic *C. pasteurianum* Fd did not significantly increase its thermostability. The reduction potential of synthetic histidine-2 Fd was −343 and −394 mV at pH 6.4 and 8.7, respectively, versus standard hydrogen electrode. Similarly, *Clostridium thermosaccharolyticum* Fd which naturally contains histidine-2 was previously determined to have a pH-dependent reduction potential [Smith, E. T., & Feinberg, B. A. (1990) *J. Biol. Chem. 265*, 14371-14376]. An electrostatic model was used to calculate the observed change in reduction potential with pH for a homologous ferredoxin with a known X-ray crystal structure containing a hypothetical histidine-2. In contrast, the reduction potential of both native *C. pasteurianum* Fd and synthetic Fd with the *C. pasteurianum* sequence was −400 mV versus standard hydrogen electrode and was pH-independent [Smith, E. T., Feinberg, B. A., Richards, J. H., & Tomich, J. M. (1991) *J. Am. Chem. Soc. 113*, 688-689]. On the basis of the above results, we conclude that the observed pH-dependent reduction potential for both synthetic and native ferredoxins that contain histidine-2 is attributable to the electrostatic interaction between histidine-2 and iron-sulfur cluster II which is approximately 6 Å away.

The ubiquitous iron-sulfur proteins play essential roles in respiratory, photosynthetic, and fermentative pathways. The electron-transport proteins ferredoxins (Fds)[1] contain [4Fe-4S] clusters that each accept or donate one electron and have a reduction potential of about −400 mV. The ferredoxin (Fd) from *Clostridium pasteurianum*, which was first isolated by Mortenson et al. (1962), is characteristic of other clostridial Fds in that it contains two [4Fe-4S] clusters and has a low molecular weight (6000).

In the elegant work by Rabinowitz and co-workers, semisynthetic procedures were used to chemically substitute or delete specific amino acids near the polypeptide terminus of *Clostridium acidi-urici* ferredoxin (Lode et al., 1974a,b, 1976). The semisynthetic approach was used to demonstrate that the

† This research was supported by a grant to B.A.F. from the National Institutes of Health (GM41927-01) and with funds from the University of Wisconsin—Milwaukee Graduate School.
* To whom correspondence should be addressed.
‡ The University of Wisconsin—Milwaukee.
§ Childrens Hospital of Los Angeles.
∥ California Institute of Technology.

[1] Abbreviations: Fd, ferredoxin, DTT, dithiothreitol; IPA, isopropyl alcohol; *t*-Boc, *tert*-butoxycarbonyl; PAGE, polyacrylamide gel electrophoresis; EPR, electron paramagnetic resonance; SHE, standard hydrogen electrode.

0006-2960/91/0430-11669$02.50/0